ASTFE
American Society
of Thermal and Fluids Engineers

8th Thermal and Fluids Engineering Conference (TFEC)
May, 2023
Partially Online Virtual and at University of Maryland, MD Conference

TFEC-2023-46263

--

BOILING ENHANCEMENT USING WATER JET IMPINGEMENT ON POROUS MEDIA COLUMNAR POST SURFACE

William A. Bevan[a],Gisuk Hwang[b], Kyosung Choo[a*]

[a]Department of Mechanical Engineering, Youngstown State University, Youngstown, OH 44555, USA
[b]Department of Mechanical Engineering, Wichita State University, Wichita, KS 67260, USA

ABSTRACT

Heat transfer and fluid flow characteristics of a submerged impinging jet in a pool boiling setup are experimentally investigated. Limited critical heat flux (CHF) and heat transfer coefficient (HTC), brought on by the counterflow of liquid and vapor across the heated surface, are the main difficulties in saturated pool-boiling heat transfer. Using porous mediums, i.e., columnar post wick, in conjunction with an impinging jet, improvements in the CHF and HTC were obtained by controlling the liquid and vapor flow for effective phase separation. The columnar post wick was fabricated using 200 μm copper particles, and the working fluid for both the pool boiling and impinging jet was water at ambient pressure. The impinging jet utilized Reynolds numbers of $800 \leq Re_w \leq 1{,}700$. The results show that in the basic pool-boiling setup, the columnar post wick provides a 63% increase in CHF enhancement when compared to the plain surface. This was done by reducing the hydrodynamic instability (Rayleigh-Taylor) wavelength. By adding an impinging jet, CHF enhancements of the columnar post wick increased by 60%, 35%, and 41% when compared to the plain surface at three different flow rates. With the potential to be used in cutting-edge thermal management systems, the combination of impinging jet and porous media offers key insights into simultaneous CHF and HTC advancements.

KEYWORDS: Impinging Jet, Pool-boiling, Porous Medium, Phase Separation

1. INTRODUCTION

For a variety of uses, such as miniaturized electronic cooling [1,2], renewable energy systems [3], and secure energy generation [4], pool boiling provides a passive high-heat flow cooling method with a low-temperature gradient. The primary technical difficulties, however, are a low heat transfer coefficient (HTC) caused by an early surface dry-out and a restricted capacity for heat evacuation or Critical Heat Flux (CHF). On a flat surface, the Rayleigh-Taylor instability wavelength, which is the critical liquid-vapor hydrodynamic instability wavelength, limits the amount of liquid that may enter an evaporator. By enhancing the liquid supply to the evaporator (or vapor escape from the evaporator), various micro-/nanoscale surface engineering approaches have demonstrated improvements in CHF and HTC. These approaches include rough surfaces, random porous matrices, microchannels/grooves, foams, mesh-like wicks, uniform porous coatings, nanostructures, and hybrid micro-/nanostructures [7-14].

The performance of the pool boiling using n-pentane was evaluated by Hwang and Kaviany. They found that different uniform microporous coatings employing sintered copper particles with varying particle sizes and different kinds of copper particles significantly improved HTC and doubled CHF [15]. They have come to the conclusion that the uniform microporous coatings' enhanced CHF is due to a shorter hydrodynamic instability wavelength, whereas varied particle types may alter HTC. Nasersharifi, Kaviany, and Hwang studied pool-boiling enhancement using multilevel modulated wicks in n-pentane. They found that by employing both a monolayer wick and a columnar post wick, CHF enhancements increased by 20% and 65%, respectively, when

*Corresponding Author: kchoo@ysu.edu

compared to a plain surface [16]. These enhancements were achieved by reducing the hydrodynamic instability wavelength.

In conjunction with porous mediums, jet impingement is another heat transfer enhancement research area. Due to their high rates of surface heating, cooling, and drying, impinging jets are often employed in a variety of technical applications. Turbine blade cooling, electronic equipment cooling, metal annealing, and textile drying are a few common industrial uses for impinging jets. Friedrich, Glaspell, and Choo studied the effect of volumetric quality on heat transfer characteristics of air-assistant jet impingement. They found that by increasing the volumetric fraction, an increase in the Nusselt number is obtained along with a new correlation for the normalized Nusselt number [17]. Choo, Friedrich, Glaspell, and Schilling studied the nozzle-to-plate spacing heat transfer effects of submerged impinging jets. They found that the normalized stagnation Nusselt number could be divided into three regions. It was found that the first region, the jet deflection region, obtained the highest Nusselt number due to the decreased nozzle-to-plate spacing and increased pumping power, while the latter two regions saw a decrease in the Nusselt number when nozzle-to-plate spacing was increased [18].

The purpose of this study is to determine the heat transfer enhancements of a columnar post wick in a pool-boiling setup subjected to an impinging jet. CHF measurements were analyzed and compared to a plain surface for a basic pool-boiling setup and a pool-boiling setup with impinging jet. Based on the experimental results, CHF enhancements were achieved with the columnar post wick in pool-boiling. By adding an impinging jet, both plain surface and columnar post wick saw CHF enhancements.

2. EXPERIMENTAL APPARATUS AND PROCEDURES

2.1 Wick Fabrication

Figure 1 shows a schematic of the plain surface and columnar post wick utilized for this experiment and their behavior in pool boiling. The plain surface was fabricated using a commercially available, thin copper disk that measured 38.17 mm in diameter and had a thickness of 0.86 mm. Measuring the instability wavelength for the plain surface, λ_p is the same as the critical Rayleigh-Taylor wavelength.

The columnar post wick utilizes the same commercially available copper disk as the plain surface. Copper particles of diameter 200 µm make up the monolayer and columnar post structure. The particular columnar post used for this experiment had a pitch distance, l_p, of 1 mm, post height of 2 mm, and a post diameter of 2.5 mm. With the addition of the columnar post comes a change in the instability wavelength. The instability wavelength equals the pitch distance of the columnar post. Fabrication of the columnar post wick consists of placing the copper sintered particles into a mold and placing the copper disk atop the copper particles. Next, the columnar post wick was placed into an argon furnace for two hours at 950°C. After two hours, the columnar post was cooled via natural convection to ambient temperature.

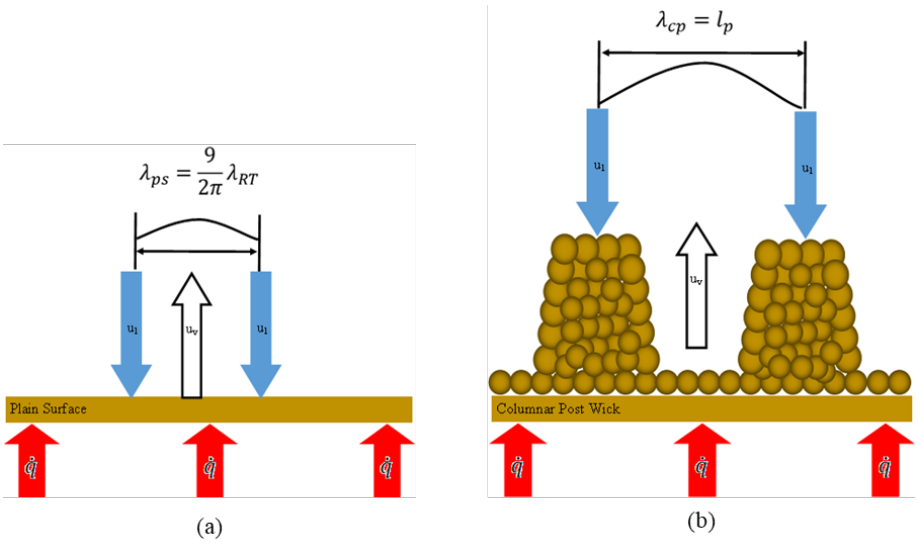

Fig 1. Schematic of the plain surface (a) and columnar post wick (b) in pool boiling

2.2 Pool-boiling setup and measurement

Figure 2 shows a schematic of the experimental apparatus. To keep the temperature gradient at a minimum when the impinging jet was in use, an Omega HCTB-3020 circulating hot temperature bath was used. From the hot water bath, flexible tubing was used to connect a Dwyer variable flow meter. The Dwyer variable flow meter, model number RMA-33-SSV, had an operating range of 0-120 cc/min. From the flow meter, more flexible tubing was used to connect the nozzle. The nozzle used for this experiment was an IDEX Health and Science stainless steel nozzle. The nozzle measured 100 mm in length, with an outer diameter of 1.60 mm, an inner diameter of 1 mm, and a thickness of 0.3 mm. The nozzle was mounted on a custom-built stand placed above the heater apparatus. The nozzle was placed above the impinging surface with a H/d value of 7. To create the pool for the pool-boiling setup, an acrylic tube was cut measuring 6.35 cm and adhered to the top of the heater apparatus using silicon.

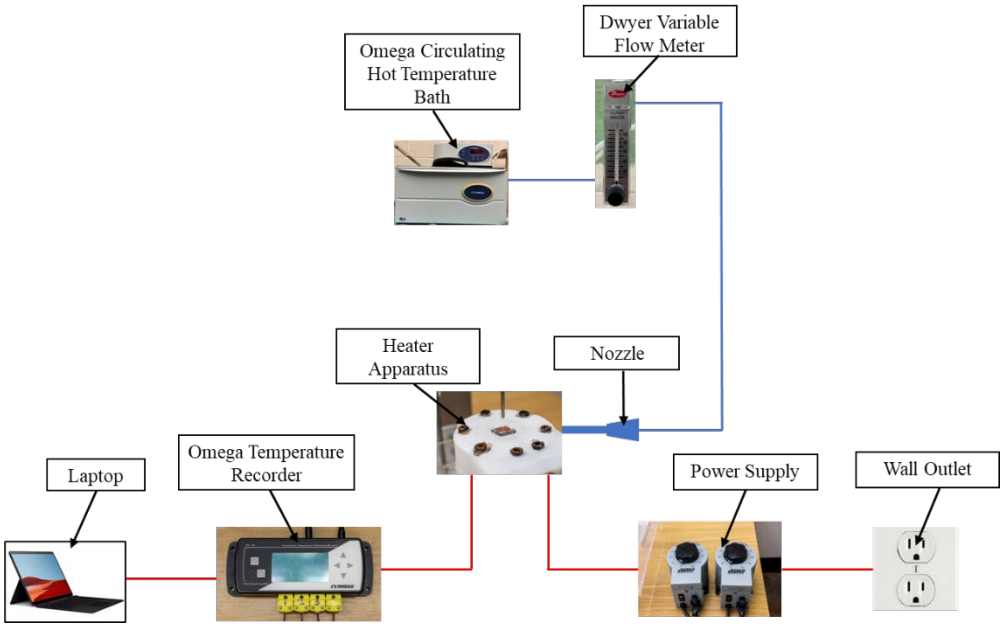

Fig 2. Schematic diagram of experimental setup

The heater was manufactured from machined copper that housed six Tutco CH43810HW cartridge heaters. These cartridge heaters were then connected in series to two Staco Energy 3PN10101B variable transformers. To keep a well-insulated test section, the copper heater was housed in machined PTFE Teflon. Used to fill in the gaps between the copper heater and PTFE Teflon were pieces of insulation layer. Atop the copper base block was another copper section that housed two K-type thermocouples that were spaced 20 mm apart from each other. Atop this copper section is the impinging surface, which housed the plain surface and columnar post wick. A solder joint was fabricated to ensure good contact between the top of the copper section and the plate/ wick. The thermocouples were then plugged into an Omega OM-CP-QuadTemp2000 temperature data recorder. To monitor the whole process, a laptop with data logger software was used.

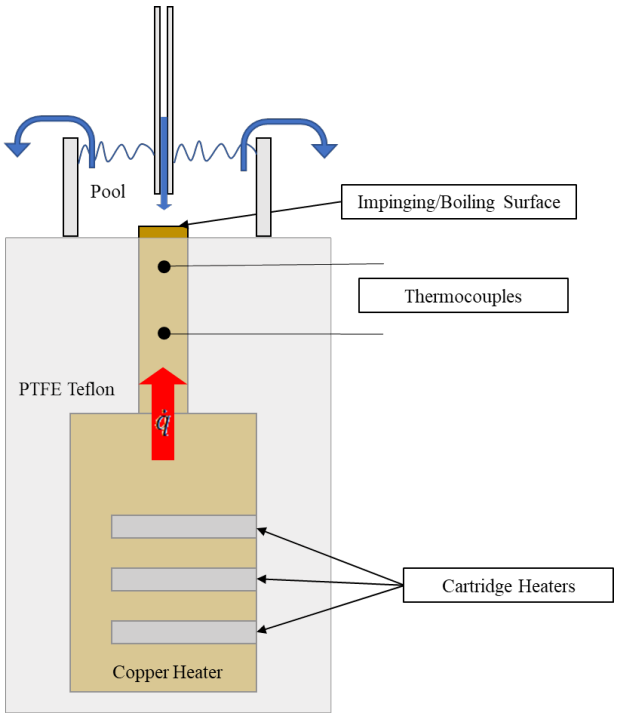

Fig 3. Test section configuration for pool-boiling with impingement jet

A schematic of the test section is presented in Figure 3. The test section was placed atop a fabricated acrylic housing that allowed for the outflow of the test section to drain properly. For the zero flow rate boiling experiment, the procedure is as follows. First, the acrylic cylinder was filled with water, and the two Staco Energy transformers were turned on. Plastic was then placed over the top of the acrylic cylinder to negate heat loss. From there, the applied heat flux was increased until bubble generation. Once bubble generation occurred, steady-state conditions had to be met until the temperature variation was ±0.5°C for a time interval of 10 minutes. Once steady state had occurred, data collection happened in 10-minute intervals. Next, critical heat flux was met when the temperature difference between the impinging surface and the saturation temperature was ~30°C or when surface dry-out was present. Once critical heat flux was obtained, the experiment was halted. This procedure was conducted for the plain surface and columnar post wick surfaces. For the impinging jet experiments, the Omega circulating hot temperature bath was turned on and set to 90°C. Once the circulating bath reached 90°C, the flow rate was set to the desired position, and the two Staco Energy variable transformers were turned on. Again, the applied heat flux was increased until bubble generation. The rest of the procedure follows the same as previously stated for both plain and wick surfaces.

The generated heat flux on the impinged surface is obtained from the conduction equation given below

$$\dot{q} = k_{copper} \frac{(T_1 - T_2)}{L_1} \tag{1}$$

The impinged surface temperature is calculated using the following equation

$$T_s = T_1 - \dot{q} \frac{L_2}{k_{copper}} \tag{2}$$

where T_1 and T_2 are the temperatures reading from the top and bottom thermocouples, $\dot{q}$ is the calculated heat flux, L_1 is the distance of the two thermocouples, L_2 is the distance of the top thermocouple to the impinged surface, and k_{copper} is the thermal conductivity of copper.

3. RESULTS AND DISCUSSION

3.1 Validation

The experimental data of the present study for a basic pool-boiling setup were compared with the empirical correlation of Warren M. Rohsenow [5,6] as a validation process. The adopted empirical correlation of Warren M. Rohsenow is seen in Equation 1. The Rohsenow correlation was plotted with ±20% uncertainty to allow for experimental error in the present study, which is present in Figure 4. Error bars are present for the ΔT_{excess} measurements. This is due to the measurements in the surface temperature needed to calculate ΔT_{excess}. All errors calculated were less than 5%.

$$\dot{q}_{nucleate} = \mu_l h_{fg} [\frac{g(\rho_l - \rho_v)}{\sigma}]^{0.5} [\frac{c_{pl}(T_s - T_{sat})}{C_{sf} h_{fg} Pr_l^n}]^3 \quad (3)$$

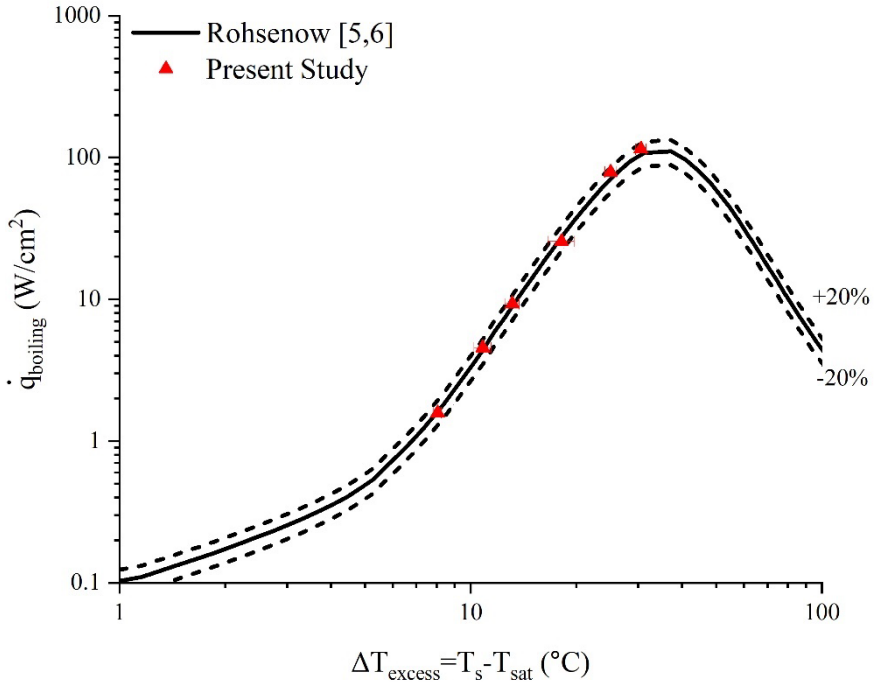

Fig 4. Correlation and comparison of pool-boiling experiment.

3.2 Critical heat flux enhancements

Figure 5 shows the boiling curves of both the plain surface and columnar post wick with their respective flow rates. Looking at a Reynolds number of zero, no impinging jet, the columnar post wick developed the highest CHF. With a pitch distance l_p=1 mm, the ΔT_{excess} is significantly reduced, allowing for a gradual increase in heat flux. Though the columnar post wick has the thickest wick structure, which is expected to increase the ΔT_{excess} through a larger conduction resistance, this is not the case. The modulation of the columnar post-wick structure allows for a significant decrease in the ΔT_{excess}. The CHF enhancements of the columnar post wick are related to the decrease in hydrodynamic instability wavelength. This means a finer bubble generation, reducing the vapor generation and prohibiting surface dry-out. This dry-out is present in the plain surface. The polished surface of the plain surface allows for a greater hydrodynamic instability wavelength which increases the vapor generation and causes rapid boiling.

When adding an impinging jet to the boiling experiment, the CHF is higher for both plates. For the plain surface, by adding an impinging jet, the flow impinges the boiling surface disrupting bubble generation. Surface dry-out is avoided by reducing the vapor phase and preventing bubble formation. By avoiding this surface dry-out, the CHF was increased. By the reduced hydrodynamic instability wavelength of the columnar post wick having an influence on the increase of CHF, the impinging jet added to this benefit. The impinging jet was able to whisk the bubble creation away due to the finer bubble generation in the columnar post wick, once again decreasing the vapor phase of the boiling phenomena. These two factors working together increased the CHF.

The last result looked at was the Reynolds number influence on the critical heat flux for both the plain surface and columnar post wick. It is seen in the figures that the Reynolds number has a significant influence on the CHF during boiling. Looking at the plain surface, by adding an impinging jet and increasing the flow rate, the CHF is further increased. This is due to the increase in fluid contact with the impinging surface and reducing the vapor phase. By reducing the vapor phase of boiling, the impinging jet reduces surface dry-out of the impinging surface. By reducing the chance for surface dry-out, the ΔT_{excess} is reduced, which further increases the CHF by keeping fluid contact with the impinging surface.

Lastly, another major CHF enhancement is present with the columnar post wick with an added impinging jet. By adding the impinging jet, the flow field is allowed to travel between those posts and sweep the bubble generation away. This reduces the vapor phase and allows for more fluid contact between the columnar post. The columnar post wick's geometry, as well as the additional impinging jet, have a significant impact on the CHF enhancement.

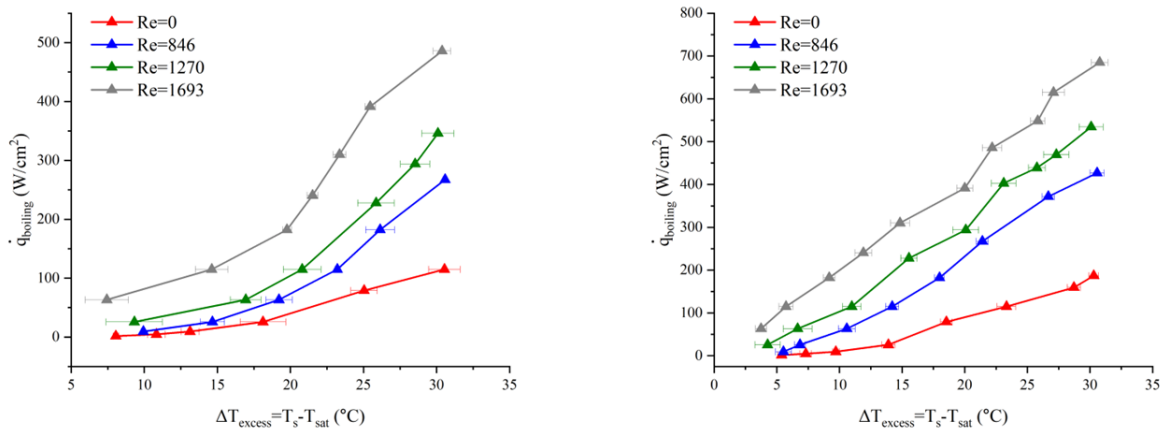

Fig 5. Reynolds number influence on boiling curves (a) plain surface (b) columnar post wick

6. CONCLUSIONS

In the present study, heat transfer characteristics of an impinging jet on a columnar post wick in pool-boiling are experimentally investigated. The effects of different flow rates, $800 \leq Re_w \leq 1{,}700$, on a plain surface and columnar post wick surface and the CHF enhancements in pool-boiling were considered.

It was found that by employing a columnar post wick in pool-boiling, CHF enhancements occurred when compared to the plain surface. By employing post structures, the columnar post wick is able to control the hydrodynamic instability wavelength through a post pitch of 1 mm and reduce the wick superheat. The columnar post wick saw a CHF enhancement of 186.9 W/cm^2 which is a 62.8% increase when compared to the plain surface. An impinging jet was added to the pool boiling configuration, which further improved CHF.

Both the plain surface and columnar post wick saw CHF enhancements under a low flow rate impinging jet. The aid of the impinging jet increases fluid contact in both plates which prohibits surface dry-out and further increase the CHF. At the lowest flow rate, the plain surface and columnar post wick saw an increase of 132.8% and 128.4%, respectively, in CHF enhancements when compared to the basic pool boiling setup. At the highest flow rate, the plain surface and columnar post wick saw an increase of 323.1% and 266.6%, respectively, in CHF enhancements when compared to the basic pool boiling setup.

NOMENCLATURE

d	Nozzle diameter	(mm)	T_s	Surface temperature	(°C)
g	Gravity constant	(m/s^2)	T_{sat}	Saturation temperature	(°C)
H	Nozzle-to-plate spacing	(mm)	T_{excess}	Excess temperature	(°C)
h_{fg}	Enthalpy of Vaporization	(kJ/mol)	u_l	Liquid velocity	(m/s)
l_p	Post pitch distance	(mm)	u_g	Vapor velocity	(m/s)
$q_{boiling}$	Boiling heat flux	(W/cm^2)	λ	Instability wavelength	(mm)
$q_{nucleate}$	Nucleate heat flux	(W/cm^2)	ρ_l	Liquid density	(kg/m^3)
Re_w	Water Reynolds number		ρ_g	Vapor density	(kg/m^3)
			σ	Surface tension of liquid-vapor interface	

REFERENCES

[1] Agostini, B., Fabbri, M., Park, J.E., Wojtan, L., Thome, J.R. and Michel, B., "State of the art of high heat flux cooling technologies." *Heat transfer engineering*, *28*(4), pp.258-281, (2007).

[2] Mudawar, I., and T. M. Anderson. "Optimization of enhanced surfaces for high flux chip cooling by pool boiling." 89-100. (1993).

[3] Chaudhry, H.N., Hughes, B.R. and Ghani, S.A., "A review of heat pipe systems for heat recovery and renewable energy applications." *Renewable and Sustainable Energy Reviews*, *16*(4), pp.2249-2259, (2012).

[4] Lahey, R.T., Moody, F.J., "The thermal hydraulics of a boiling nuclear reactor." (1977).

[5] Rohsenow, W.M., "A method of correlating heat transfer data for surface boiling of liquids," Trans. Am. Soc. Mech. Eng. 74 969-975, (1952).

[6] Rohsenow, W.M., Griffith, P., "Correlation of maximum heat flux data for boiling of saturated liquids," Chem. Eng. Prog. 52 47. (1956).

[7] Kurihara, H.M. and Myers, J.E., "The effects of superheat and surface roughness on boiling coefficients." *AIChE Journal*, *6*(1), pp.83-91. (1960).

[8] Wang, J. and Catton, I., "Enhanced evaporation heat transfer in triangular grooves covered with a thin fine porous layer." *Applied Thermal Engineering*, *21*(17), pp.1721-1737. (2001).

[9] Das, A.K., Das, P.K. and Saha, P., "Performance of different structured surfaces in nucleate pool boiling." *Applied Thermal Engineering*, *29*(17-18), pp.3643-3653. (2009).

[10] Jin, L.W., Leong, K.C. and Pranoto, I., "Saturated pool boiling heat transfer from highly conductive graphite foams." *Applied Thermal Engineering*, *31*(14-15), pp.2685-2693. (2011).

[11] Nakayama, W., Daikoku, T., Kuwahara, H. and Nakajima, T., "Dynamic model of enhanced boiling heat transfer on porous Surfaces"—Part II: Analytical modeling. (1980).

[12] Rainey, K.N. and You, S.M., "Pool boiling heat transfer from plain and microporous, square pin-finned surfaces in saturated FC-72." *J. Heat Transfer*, *122*(3), pp.509-516. (2000).

[13] Lu, Y.W. and Kandlikar, S.G., "Nanoscale surface modification techniques for pool boiling enhancement—a critical review and future directions." *Heat Transfer Engineering*, *32*(10), pp.827-842. (2011).

[14] Dhillon, N.S., Buongiorno, J. and Varanasi, K.K., "Critical heat flux maxima during boiling crisis on textured surfaces." *Nature communications*, *6*(1), pp.1-12. (2015).

[15] Hwang, G.S. and Kaviany, M., "Critical heat flux in thin, uniform particle coatings." *International journal of heat and mass transfer*, *49*(5-6), pp.844-849. (2006).

[16] Nasersharifi, Y., Kaviany, M. and Hwang, G., "Pool-boiling enhancement using multilevel modulated wick." *Applied Thermal Engineering*, *137*, pp.268-276. (2018).

[17] Friedrich, B.K., Glaspell, A.W. and Choo, K., "The effect of volumetric quality on heat transfer and fluid flow characteristics of air-assistant jet impingement." *International Journal of Heat and Mass Transfer*, *101*, pp.261-266. (2016).

[18] Choo, K., Friedrich, B.K., Glaspell, A.W. and Schilling, K.A., "The influence of nozzle-to-plate spacing on heat transfer and fluid flow of submerged jet impingement." *International Journal of Heat and Mass Transfer*, *97*, pp.66-69. (2016).